A Novel Voltage Reconstruction Method for MRAS based Sensorless IPMSM Drives

Xu, Junzhong; Soeiro, Thiago B.; Wang, Yong; Wu, Yang; Tang, Houjun ; Bauer, Pavol

DOI
10.1109/PEMC48073.2021.9432573

Publication date
2021

Document Version
Final published version

Published in
Proceedings - 2021 IEEE 19th International Power Electronics and Motion Control Conference, PEMC 2021

A Novel Voltage Reconstruction Method for MRAS based Sensorless IPMSM Drives

Junzhong Xu[1], Thiago Batista Soeiro[2], Yong Wang[1], Yang Wu[2], Houjun Tang[1], Pavol Bauer[2]
1: *Department of Electrical Engineering, Shanghai Jiao Tong University*, Shanghai, China
2: *DCE&S group, Delft University of Technology*, Delft, The Netherlands
Junzhongxu@sjtu.edu.cn, T.BatistaSoeiro@tudelft.nl, Wangyong75@sjtu.edu.cn, Y.Wu-6@tudelft.nl,
Hjtang@sjtu.edu.cn, P.Bauer@tudelft.nl

2021 IEEE 19th International Power Electronics and Motion Control Conference (PEMC) | 978-1-7281-5660-6/20/$31.00 ©2021 IEEE | DOI: 10.1109/PEMC48073.2021.9432573

***Abstract*—Different advanced sensorless techniques have been proposed based on the model reference adaptive system (MRAS) principle to make the interior permanent magnet synchronous motor (IPMSM) drives mechanically more robust. However, in the special application such as high-power traction systems, the difference between the switching frequency and the calculation frequency is large, and the inconsistency between the command voltage and the actual voltage will affect the accuracy of the MARS estimator. To overcome such a drawback, this paper proposes a novel voltage reconstruction method to improve the accuracy of the MRAS estimator. Simulations and experiments are conducted to verify the effectiveness of the proposed method. Combining with the proposed algorithm, the problem of the inconsistency can be solved, and an accurate rotation estimation can be realized.**

***Index Terms*—Model Reference Adaptive System (MRAS), Sensorless, Interior Permanent Magnet Synchronous Motor (IPMSM), Voltage Reconstruction, Switching Frequency, Calculation Frequency.**

I. Introduction

Interior permanent magnet synchronous motor (IPMSM) has established increasing popularity in high-power traction systems for its higher efficiency and wider speed range operations [1]. Presently, the primary concern of high-power traction systems is associated with its reduced reliability caused by position sensors, which have accounted for many system failures [2]. Therefore, for reliability improvement as well as cost reduction, significant efforts have been carried out in IPMSM drives to estimate the machine speed without position sensors, which are referred as sensorless control and have been a hot research focus for years [3]–[7].

Various advanced techniques have been proposed in the literature to make the sensorless IPMSM drives mechanically more stable. Such approaches can be broadly divided into two main categories: signal injection-based and model-based methods. Based on the types of injection signals, signal injection-based methods can be roughly classified into rotating injection [3], pulsating injection [4], and square-wave injection [5]. Although these methods are insightful and achieve a marked effect in obtaining an accurate rotor position, the audible noise caused by the injected signal is often harsh to hear [3]–[5]. On the other hand, model-based methods based on the mathematical model of the motor are well used in medium- and high-speed operation [6]–[9]. The model-based method is based on the principle of model reference adaptive system (MRAS), where an error vector is formed from the outputs of two models, both dependent on different motor parameters [6]. MRAS-based methods, including rotor-flux MRAS, back EMF MRAS, reactive power MRAS, and stator current MRAS are divided according to how the error signal is calculated [7]. Currently, MRAS-based methods are preferable due to their relatively simpler algorithm.

However, most of the aforementioned MRAS-based approaches need the information of the fundamental phase voltage and thus become less effective under low switching frequency, which is a significant issue in high-power traction systems [10]. Since the fundamental phase voltage cannot be measured directly, command voltage is usually applied instead of the actual one. Nevertheless, due to the undesirable characteristics of inverters [11], it is hard to make the command voltage exactly the same as the actual one. Although dead-time compensation strategy in [11] and a current-control scheme in [12] can be applied to relieve the influence of voltage disturbance and improve the accuracy of speed estimation, the validity of both methods is still limited in high-power traction system [13]. Additionally, discrete-time full-order observers proposed in [2], [14] enable the position estimation of IPMSM to operate at low switching frequency but inevitably increase the computational burden. Therefore, a flexible solution with lower system complexity is worthy of promotion in practice to overcome the problem of inconsistency between command voltage and actual voltage, while realizing the accurate estimation of rotor position and speed.

The main contribution of this paper is that a novel voltage reconstruction algorithm is proposed for sensorless IPMSM drives to improve the accuracy of rotor position and speed estimation based on stator-current MRAS in a high-power application, which is usually operated under low switching frequency. Realized through digital control units, the proposed algorithm is simple in practice. The rest of the paper is organized as follows. Firstly, the mathematical models of the IPMSM and MRAS estimator are established. Then, the defect of traditional method operating under low-switching frequency condition is analyzed. Thereafter, the proposed voltage reconstruction algorithm is described to overcome the inconsistency between command voltage and actual voltage. Finally, the effectiveness of the proposed method is validated by both simulation and experiments.

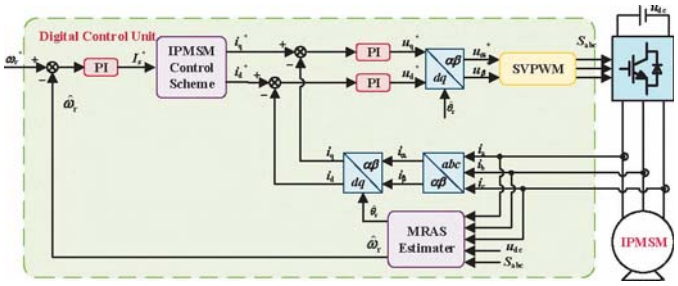

Fig. 1. Model-based sensorless IPMSM drive.

II. Mathematical Principle of Sensorless IPMSM Drive Based on MRAS Estimator and the Defect of Traditional Method

A. Mathematical Model and Vector Control Scheme of the Sensorless IPMSM

The IPMSM is mathematically modeled in the d-q rotating reference frame. The d-axis is oriented along the permanent magnet flux, and the q-axis is created by rotating the d-axis 90 degrees counterclockwise. The stator voltage and flux equation can be expressed as:

$$\begin{cases} u_d = R_s i_d + \frac{\mathrm{d}\psi_d}{\mathrm{d}t} - \psi_q \omega_r \\ u_q = R_s i_q + \frac{\mathrm{d}\psi_q}{\mathrm{d}t} + \psi_d \omega_r \end{cases} \tag{1}$$

$$\begin{cases} \psi_d = L_d i_d + \psi_f \\ \psi_q = L_q i_q \end{cases} \tag{2}$$

where u_d, u_q, i_d, and i_q are the stator voltages and currents respectively; R_s is the stator resistance; L_d and L_q are the $d-q$ axis inductances; ψ_d and ψ_q are the $d-q$ axis stator magnetic flux; $\omega_r = \frac{\mathrm{d}\theta_r}{\mathrm{d}t}$ is the rotor electrical angular speed, and ψ_f is the permanent magnet flux. The equations (1) and (2) can be presented into matrix form as:

$$\frac{d}{dt}\begin{bmatrix} i_d \\ i_q \end{bmatrix} = \begin{bmatrix} -\frac{R_s}{L_d} & \frac{L_q}{L_d}\omega_r \\ -\frac{L_d}{L_q}\omega_r & -\frac{R_s}{L_d} \end{bmatrix}\begin{bmatrix} i_d \\ i_q \end{bmatrix} + \begin{bmatrix} \frac{u_d}{L_d} \\ \frac{u_q}{L_q} - \frac{\omega_r}{L_q}\psi_f \end{bmatrix} \tag{3}$$

Thereafter, electromagnetic torque T_e can be obtained based on the number of pole pairs p of the IPMSM:

$$T_\mathrm{e} = \frac{3p}{2}\left[\psi_f i_q + (L_d - L_q) i_d i_q\right] \tag{4}$$

Fig. 1 shows the vector control scheme of the sensorless IPMSM drive based on the MRAS Estimator. Different vector control schemes including unit power factor ($\cos\varphi = 1$) control, $i_d = 0$ control, and maximum torque per ampere (MTPA) control can be chosen to optimize the IPMSM control.

B. Sensorless Stator-Current Based MRAS Estimator

The actual motor can be considered as a reference model of MRAS estimator, where the stator current can be calculated based on the voltage and flux models in (1) and (2), and rewritten in (5) as follows:

$$\frac{d}{dt}\begin{bmatrix} i_d + \frac{\psi_f}{L_d} \\ i_q \end{bmatrix} = \begin{bmatrix} -\frac{R_s}{L_d} & \frac{L_q}{L_d}\omega_r \\ -\frac{L_d}{L_q}\omega_r & -\frac{R_s}{L_d} \end{bmatrix}\begin{bmatrix} i_d + \frac{\psi_f}{L_d} \\ i_q \end{bmatrix} + \begin{bmatrix} \frac{u_d}{L_d} + \frac{R_s\psi_f}{L_d} \\ \frac{u_q}{L_q} \end{bmatrix} \tag{5}$$

To conveniently analyze the system, the system matrices are introduced as in (6) and (7):

$$\mathbf{A} = \begin{bmatrix} -\frac{R_s}{L_d} & \frac{L_q}{L_d}\omega_r \\ -\frac{L_d}{L_q}\omega_r & -\frac{R_s}{L_d} \end{bmatrix} \tag{6}$$

$$\mathbf{B} = \begin{bmatrix} \frac{1}{L_d} & 0 \\ 0 & \frac{1}{L_q} \end{bmatrix} \tag{7}$$

Then, the modified stator current and voltage vectors are defined:

$$\mathbf{i_s} = \begin{bmatrix} i_d' \\ i_q \end{bmatrix} = \begin{bmatrix} i_d + \frac{\psi_f}{L_d} \\ i_q \end{bmatrix} \tag{8}$$

$$\mathbf{u_s} = \begin{bmatrix} u_d' \\ u_q \end{bmatrix} = \begin{bmatrix} u_d + R_s\psi_f \\ u_q \end{bmatrix} \tag{9}$$

Thus, the reference model can be described as:

$$\dot{\mathbf{i}}_\mathbf{s} = \mathbf{A}\mathbf{i_s} + \mathbf{B}\mathbf{u_s} \tag{10}$$

In order to simplify the IPMSM model in the position sensorless drive system, the error of the rotor position is ignored in this paper, which means that the IPMSM model in the rotating $d-q$ frame can be directly employed to estimate the rotor position and speed [15]. The rotor speed is used as the parameter of adjustable model to make the parameter-current error between two models turn to zero according to the adaptation mechanism. After that, the estimation value $\hat{\omega}_r$ can be regarded as a correct speed ω_r. The speed estimation can be described as follows:

$$\frac{d}{dt}\begin{bmatrix} \hat{i}_d' \\ \hat{i}_q \end{bmatrix} = \begin{bmatrix} -\frac{R_s}{L_d} & \frac{L_q}{L_d}\hat{\omega}_r \\ -\frac{L_d}{L_q}\hat{\omega}_r & -\frac{R_s}{L_d} \end{bmatrix}\begin{bmatrix} \hat{i}_d' \\ \hat{i}_q \end{bmatrix} + \begin{bmatrix} \frac{1}{L_d} & 0 \\ 0 & \frac{1}{L_q} \end{bmatrix}\begin{bmatrix} u_d' \\ u_q \end{bmatrix} \tag{11}$$

All of the estimated parameters in (11) are marked by $\hat{}$ and it can be rewritten as:

$$\dot{\hat{\mathbf{i}}}_\mathbf{s} = \hat{\mathbf{A}}\hat{\mathbf{i}}_\mathbf{s} + \mathbf{B}\mathbf{u_s} \tag{12}$$

Subtracting (10) for the reference model from the corresponding equations for the adjustable model, the following state error equations are obtained:

$$\frac{d}{dt}\begin{bmatrix} \varepsilon_d \\ \varepsilon_q \end{bmatrix} = \begin{bmatrix} -\frac{R_s}{L_d} & \frac{L_q}{L_d}\omega_r \\ -\frac{L_d}{L_q}\omega_r & -\frac{R_s}{L_d} \end{bmatrix}\begin{bmatrix} \varepsilon_d \\ \varepsilon_q \end{bmatrix} - \begin{bmatrix} -\frac{L_q}{L_d}\hat{i}_q' \\ \frac{L_d}{L_q}\hat{i}_d' \end{bmatrix}(\hat{\omega}_r - \omega_r) \tag{13}$$

Thus,

$$\dot{\boldsymbol{\varepsilon}} = \mathbf{A}\boldsymbol{\varepsilon} - \mathbf{D}\mathbf{W} \tag{14}$$

Where, $\mathbf{W} = [-\frac{L_q}{L_d}\hat{i}_q', \frac{L_d}{L_q}\hat{i}_d']^\mathrm{T}(\hat{\omega}_r - \omega_r)$, and $\boldsymbol{\varepsilon} = [\varepsilon_d, \varepsilon_q]^\mathrm{T} = [i_d' - \hat{i}_d', i_q' - \hat{i}_q']^\mathrm{T}$. By choosing $\mathbf{D} = \mathbf{I}$, the adjustable models are linear time-varying systems. Since $\hat{\omega}_r$ is a function of the state error, these equations describe a nonlinear-feedback system as illustrated in Fig. 2. Therefore, the established MRAS estimator will be stable based on the Popov hyperstability theory [15], [16].

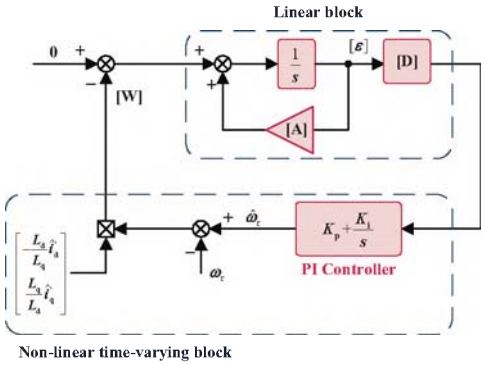

Fig. 2. Equivalent structure of the MRAS estimator.

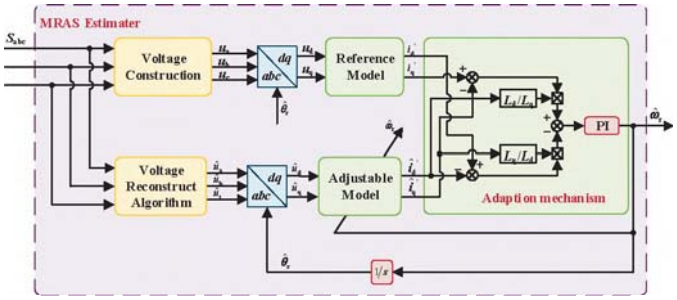

Fig. 3. Established stator-current based MRAS Estimator.

Finally, the estimated speed $\hat{\omega}_r$ can be achieved as:

$$\begin{aligned}\hat{\omega}_r =& K_{\mathrm{p}}\left[\frac{L_d}{L_q}\hat{i}_{\mathrm{d}}\left(i'_{\mathrm{q}}-\hat{i}'_{\mathrm{q}}\right)-\frac{L_q}{L_d}\hat{i}_{\mathrm{q}}\left(i'_{\mathrm{d}}-\hat{i}'_{\mathrm{d}}\right)\right]+\hat{\omega}_r(0)+\\ &\int_0^t K_{\mathrm{i}}\left[\frac{L_d}{L_q}\hat{i}_{\mathrm{d}}\left(i'_{\mathrm{q}}-\hat{i}'_{\mathrm{q}}\right)-\frac{L_q}{L_d}\hat{i}_{\mathrm{q}}\left(i'_{\mathrm{d}}-\hat{i}'_{\mathrm{d}}\right)\right]d\tau\\ =& K_{\mathrm{p}}\left[\frac{L_q}{L_d}i_{\mathrm{d}}\hat{i}_{\mathrm{q}}-\frac{L_d}{L_q}i_{\mathrm{q}}\hat{i}_{\mathrm{d}}-\left(\frac{L_q}{L_d}-\frac{L_d}{L_q}\right)\hat{i}_{\mathrm{d}}\hat{i}_{\mathrm{q}}-\right.\\ &\left.\frac{\psi_f}{L_q}\left(i_q-\hat{i}_{\mathrm{q}}\right)\right]+\int_0^t K_{\mathrm{i}}\left[\frac{L_q}{L_d}i_{\mathrm{d}}\hat{i}_{\mathrm{q}}-\frac{L_d}{L_q}i_{\mathrm{q}}\hat{i}_{\mathrm{d}}-\right.\\ &\left.\left(\frac{L_q}{L_d}-\frac{L_d}{L_q}\right)\hat{i}_{\mathrm{d}}\hat{i}_{\mathrm{q}}-\frac{\psi_f}{L_q}\left(i_q-\hat{i}_{\mathrm{q}}\right)\right]d\tau+\hat{\omega}_r(0)\end{aligned} \tag{15}$$

In the above equation, i_{d} and i_{q} are achieved by the transformation of the measured stator currents i_{a}, i_{b}; i_{c}, $\hat{i}_{\mathrm{d}}$ and $\hat{i}_{\mathrm{q}}$ are calculated through the adjustable model in (11); ψ_f can be regarded as a constant. Thus, rotor position $\hat{\theta}_r$ can be obtained by integrating the estimated speed. The established MRAS estimator is illustrated in Fig. 3. The inputs of the estimation block are the three phase command voltage derived by the switching states S_{abc} and actual current of the real motor, and the outputs are the estimated speed and position.

C. Defect of Traditional Method at Low Switching Frequency

In a digital PWM controller, the command voltage is calculated only at periodic time instants [17], [18]. Hence, sampling values can be stored in the processor memory with the modulation index as a parameter. Based on these, the switching instants can be obtained as the respective points

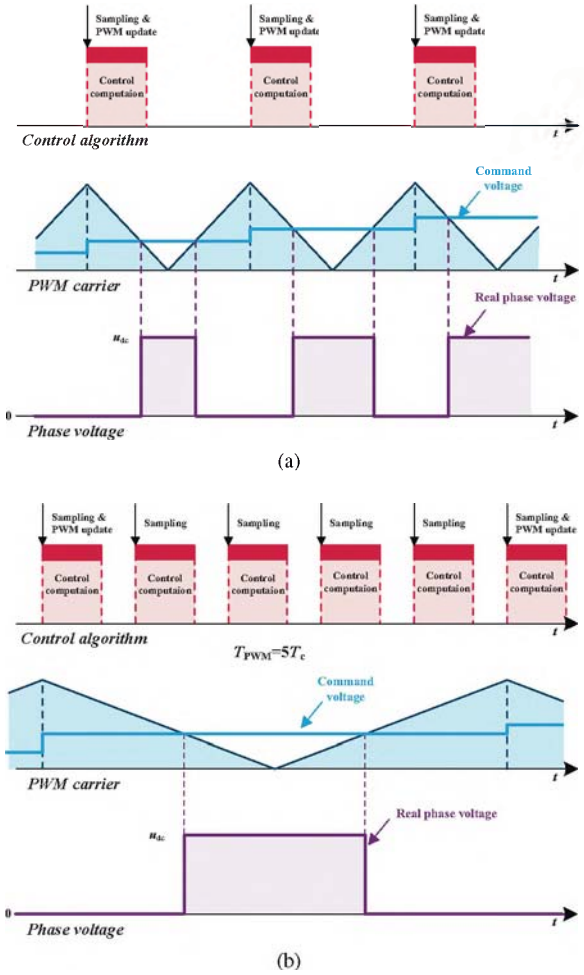

Fig. 4. Construction of the estimated voltage (a) $T_s = T_c$ (b) $T_s = 5T_c$.

where the triangular slope reaches the sampled value, as shown in Fig. 4(a). Under most conditions, command voltage u_c can be used directly in the control algorithm, because according to the area equivalent principle, command voltage u_c is exactly the same as the mean value of the real phase voltage u_r in each control computation period, as the switching frequency f_{s} is equal to the control calculation frequency f_c:

$$u_c = \overline{u_r} = \frac{\int_0^{T_{\mathrm{s}}} u_r dt}{T_{\mathrm{s}}} = \frac{\int_0^{T_{\mathrm{c}}} u_r dt}{T_{\mathrm{c}}} \tag{16}$$

However, in high-power traction systems, f_s must be set low to achieve fewer losses, which is dozens of times less than the f_c. Hence, there would be a significant error between the u_r and the u_c, if u_c is still applied into the motor control algorithm. Taking $n = 5$ as an example, as illustrated in Fig. 4(b), the existing error at the xth period is:

$$\begin{aligned}\varepsilon_x &= \frac{1}{T_{\mathrm{c}}}\int_{(x-1)T_{\mathrm{c}}}^{xT_{\mathrm{c}}} u_r dt - u_c\\ &= \begin{cases}(1-d)u_{\mathrm{dc}} & x=1,5\\ -du_{\mathrm{dc}} & x=3\\ (3d-2)u_{\mathrm{dc}}/2 & x=2,4.\end{cases}\end{aligned} \tag{17}$$

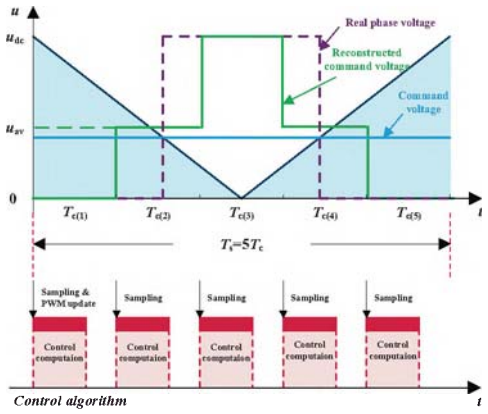

(a)

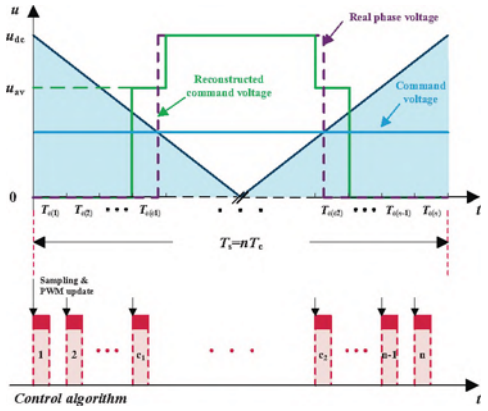

(b)

Fig. 5. Reconstruction of the estimated voltage (a) $T_s = 5T_c$ (b) $T_s = nT_c$.

Where $u_c = du_{\rm dc}$. Although $\sum_{x=1}^{5} \varepsilon_x = 0$ in each switching period, the error does exist in every calculation period, which affects the accuracy of MRAS observer and the stability of control algorithm.

III. Proposed Voltage Reconstruction Algorithm

To overcome such a significant drawback, a novel algorithm to eliminate the command voltage error under low switching frequency and high MRAS calculation frequency is proposed. As shown in Fig. 5(a), $T_{\rm s} = 5T_{\rm c}$, and transition calculation periods are T_2 and T_4, where the reconstructed command voltage is defined as $(5d-2)u_{\rm dc}/2$. Then, the reconstructed command voltage in T_1 and T_5 is set to $u_{\rm dc}$, and that in T_3 is 0. Generalizing the algorithm to general cases in Fig. 5(b), the period of transition can be first decided by:

$$\begin{cases} c_1 &= floor\left(\frac{1-d}{2}n\right)+1 \\ c_2 &= n-c_1+1 \end{cases} \tag{18}$$

Thereafter, the number of calculation periods with the value of $u_{\rm dc}$, $n_{\rm c} = c_1 - 1 + n - c_2$, is derived, which determines the value of reconstructed voltage over the xth calculation period u_x as:

$$u_x = \begin{cases} u_{\rm dc} & x < c_1 \text{ or } x > c_2 \\ (dn - n_c)u_{\rm dc}/2 & x = c_1,\ c_2 \\ 0 & c_1 < x < c_2. \end{cases} \tag{19}$$

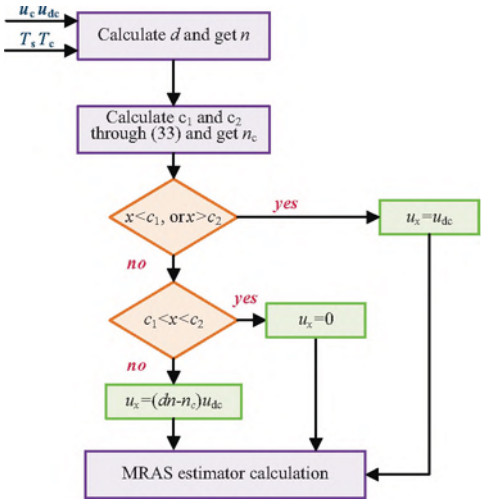

Fig. 6. Flowchart of the proposed command voltage reconstruction algorithm

The flowchart of the proposed command voltage reconstruction algorithm is shown in Fig. 6. With lower calculation burden, the algorithm is simple to apply in the practice. Consequently, the error between command voltage and actual voltage can be eliminated, and more precise information of command phase voltage will be achieved, which will improve the accuracy of the MRAS estimator.

IV. Simulation and Experimental Verification

In order to verify the effectiveness of proposed command voltage reconstruction strategy, simulations and experimental tests are conducted. Firstly, a model of PWM inverter-fed IPMSM drive system is built in MATLAB/SIMULINK platform. Then, the proposed position sensorless control has been operated on a digital-control hardware platform with ARM (STM32F743) plus Altera cpld (MAX3000A EPW3128ATC100-10N). The parameters of the IPMSM used in both simulation and experiment are listed in TABLE I.

A. Simulation Results

In the simulation system, the IPMSM is operated with position sensor and the current MRAS estimator both with and without command voltage reconstruction algorithm are used to observe the accuracy of the estimated speed.

Fig. 7 shows the change of the estimated rotor speed with the decline in MRAS calculation frequency f_c, which is set to be equal to the switching frequency. It can be seen that when $f_c = 30$ kHz, the estimated rotor speed matches well with the reference. However, it has oscillation with f_c reduced to 5 kHz, and it turns to be unstable when f_c falls into 650 Hz.

TABLE I
IPMSM PARAMETERS

Parameters	Value
Rated Power	45 kW
Rated Speed	1300 r/min
Rated Voltage	233.7 V
Rated Current	135 A
Rated Torque	331 N·m
Resistance	0.045 Ω
d-axis Inductance	0.7649 mH
q-axis Inductance	2.1374 mH
Number of pole pairs p	4
Permanent magnet flux ψ_s	0.2337 wb

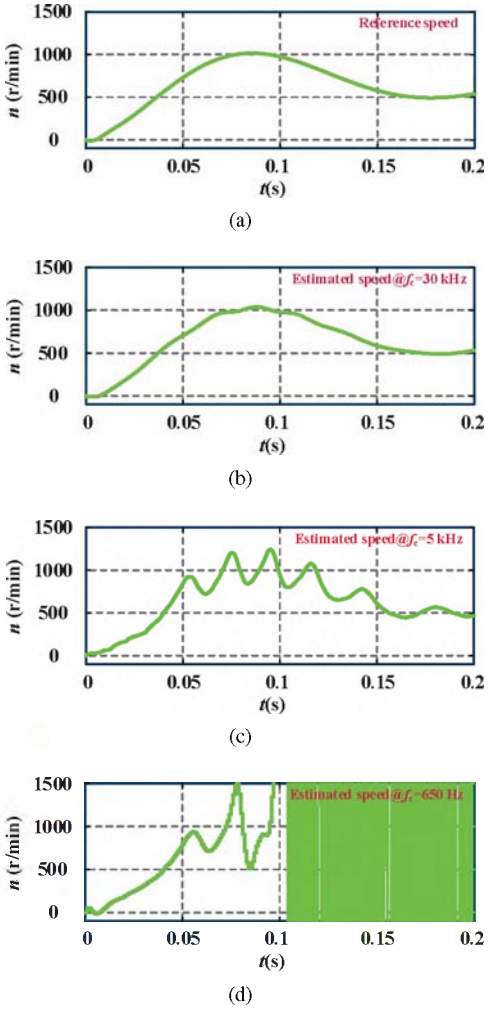

Fig. 7. Estimated rotor speed with the decline in the calculation frequency

Therefore, f_c needs to be set high to maintain the stability and the accuracy of speed estimator.

Fig. 8 shows the comparison between the estimated speed with proposed algorithm and that using the command voltage directly under $f_c = 30$ kHz and $f_s = 650$ Hz operating condition. Although both estimated results succeed in matching

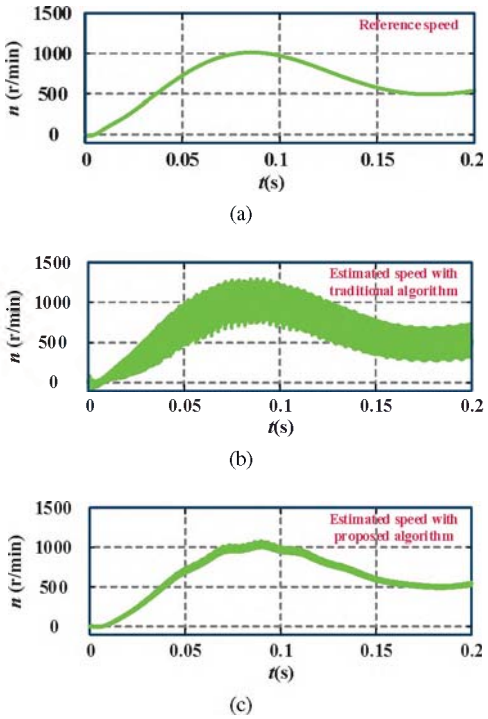

Fig. 8. Comparison between the estimated speed with common voltage command and that with the reconstructed voltage command

the reference, it is evident that the MRAS estimator with the reconstructed command voltage is more accurate. Therefore, the validity of the proposed method is verified.

B. Experimental Validity

Fig. 9 shows the steady-state control performance at 1300 r/min under 50% rated load. d- and q-axis current and estimation with reconstructed command voltage and with common command voltage are shown in Fig. 9(a) and Fig. 9(b) respectively. It can be seen that with the reconstructed command voltage, the estimated values of the d- and q-axis current track the measured values better, which is able to estimate the ripple fluctuations in current, while the other can merely estimate their mean value. As a result, the position estimation error obtained in Fig. 9(c) is much lower than that in Fig. 9(d). It is worth noting that although the MRAS estimator with common command voltage can also make the IPMSM work under low switching frequency, the increased ripple of position estimation error may affect the accuracy and stability, resulting in unexpected system fault.

V. CONCLUSION

This paper has proposed a novel voltage reconstruction algorithm to improve the accuracy of MRAS estimator for sensorless IPMSM drives, where the difference between the switching frequency and the control frequency is large. The mathematic model has shown that the inconsistency between the command voltage and the actual voltage will affect the accuracy of the MARS estimator in tradition method, which can be totally eliminated by the proposed algorithm. Finally,

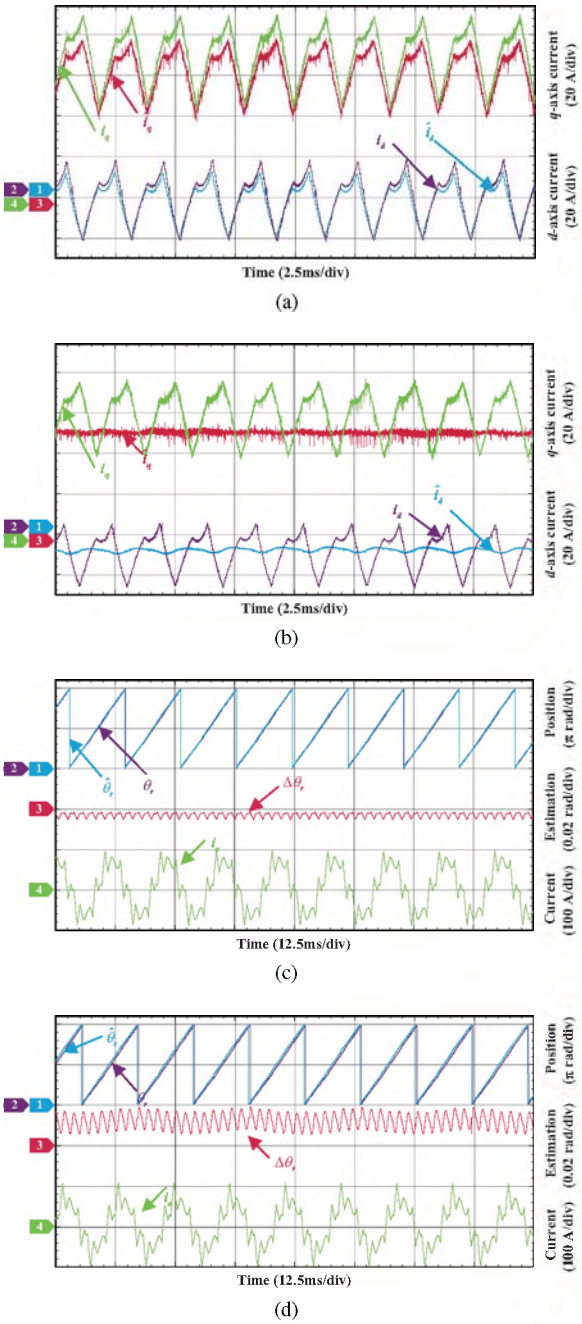

Fig. 9. Steady-state control performance at 1300 r/min under 50% rated load. (a) d- and q-axis current and estimation with reconstructed command voltage (b) d- and q-axis current and estimation with common command voltage (c) position and error with reconstructed command voltage (d) position and error with common command voltage.

both simulations and experiments have verified the effectiveness and superiority of the proposed method.

ACKNOWLEDGMENT

This work is supported in part by the scholarship from China Scholarship Council (CSC) under the Grant: *CSC NO. 201906230170*.

REFERENCES

[1] C. Calleja, A. López-de-Heredia, H. Gaztañga, L. Aldasoro, and T. Nieva, "Validation of a modified direct-self-control strategy for PMSM in railway-traction applications," *IEEE Trans. Ind. Electron.*, vol. 63, no. 8, pp. 5143–5155, Aug. 2016.

[2] S. Yin, Y. Huang, Y. Xue, D. Meng, C. Wang, Y. Lv, L. Diao, and J. Jatskevich, "Improved full-order adaptive observer for sensorless induction motor control in railway traction systems under low-switching frequency," *IEEE J. Emerg. Sel. Topics Power Electron.*, vol. in press, pp. 1–1, 2019.

[3] Q. Tang, A. Shen, X. Luo, and J. Xu, "IPMSM sensorless control by injecting bidirectional rotating HF carrier signals," *IEEE Trans. Power Electron.*, vol. 33, no. 12, pp. 10 698–10 707, Dec. 2018.

[4] Q. Tang, A. Shen, X. Luo, and J. Xu, "PMSM sensorless control by injecting HF pulsating carrier signal into ABC frame," *IEEE Trans. Power Electron.*, vol. 32, no. 5, pp. 3767–3776, May. 2017.

[5] G. Wang, D. Xiao, G. Zhang, C. Li, X. Zhang, and D. Xu, "Sensorless control scheme of IPMSMs using HF orthogonal square-wave voltage injection into a stationary reference frame," *IEEE Trans. Power Electron.*, vol. 34, no. 3, pp. 2573–2584, Mar. 2019.

[6] T. Orlowska-Kowalska and M. Dybkowski, "Stator-current-based MRAS estimator for a wide range speed-sensorless induction-motor drive," *IEEE Trans. Ind. Electron.*, vol. 57, no. 4, pp. 1296–1308, Apr. 2010.

[7] E. Dehghan-Azad, S. Gadoue, D. Atkinson, H. Slater, P. Barrass, and F. Blaabjerg, "Sensorless control of IM based on stator-voltage MRAS for limp-home EV applications," *IEEE Trans. Power Electron.*, vol. 33, no. 3, pp. 1911–1921, Mar. 2018.

[8] G. Wang, T. Li, G. Zhang, X. Gui, and D. Xu, "Position estimation error reduction using recursive-least-square adaptive filter for model-based sensorless interior permanent-magnet synchronous motor drives," *IEEE Trans. Ind. Electron.*, vol. 61, no. 9, pp. 5115–5125, Sep. 2014.

[9] G. Wang, H. Zhan, G. Zhang, X. Gui, and D. Xu, "Adaptive compensation method of position estimation harmonic error for EMF-based observer in sensorless IPMSM drives," *IEEE Trans. Power Electron.*, vol. 29, no. 6, pp. 3055–3064, Jun. 2014.

[10] L. Diao, D. Sun, K. Dong, L. Zhao, and Z. Liu, "Optimized design of discrete traction induction motor model at low-switching frequency," *IEEE Trans. Power Electron.*, vol. 28, no. 10, pp. 4803–4810, Oct. 2013.

[11] N. Urasaki, T. Senjyu, K. Uezato, and T. Funabashi, "Adaptive dead-time compensation strategy for permanent magnet synchronous motor drive," *IEEE Trans. Energy Conversion.*, vol. 22, no. 2, pp. 271–280, Jun. 2007.

[12] Y. A. I. Mohamed, "Design and implementation of a robust current-control scheme for a PMSM vector drive with a simple adaptive disturbance observer," *IEEE Trans. Ind. Electron.*, vol. 54, no. 4, pp. 1981–1988, Aug. 2007.

[13] G. Narayanan and V. T. Ranganathan, "Two novel synchronized bus-clamping PWM strategies based on space vector approach for high power drives," *IEEE Trans. Power Electron.*, vol. 17, no. 1, pp. 84–93, Jan. 2002.

[14] G. Zhang, G. Wang, D. Xu, and Y. Yu, "Discrete-time low-frequency-ratio synchronous-frame full-order observer for position sensorless IPMSM drives," *IEEE J. Emerg. Sel. Topics Power Electron.*, vol. 5, no. 2, pp. 870–879, Jun. 2017.

[15] Y. Shi, K. Sun, L. Huang, and Y. Li, "Online identification of permanent magnet flux based on extended kalman filter for IPMSM drive with position sensorless control," *IEEE Trans. Ind. Electron.*, vol. 59, no. 11, pp. 4169–4178, Nov. 2012.

[16] Y. Liang and Y. Li, "Sensorless control of PM synchronous motors based on MRAS method and initial position estimation," in *Proc. Int. Conf. Elect. Mach. Syst.*, vol. 1, pp. 96–99 vol.1, Nov. 2003.

[17] J. Xu, J. Han, Y. Wang, M. Ali, and H. Tang, "High-frequency SiC three-phase VSIs with common-mode voltage reduction and improved performance using novel tri-state PWM method," *IEEE Trans. Power Electron.*, vol. 34, no. 2, pp. 1809–1822, 2019.

[18] J. Xu, J. Han, Y. Wang, S. Habib, and H. Tang, "A novel scalar PWM method to reduce leakage current in three-phase two-level transformerless grid-connected VSIs," *IEEE Trans. Ind. Electron.*, vol. 67, no. 5, pp. 3788–3797, May. 2020.